CERTIFICATION OF APPROVAL

Mechanical and Physical Effect of Nitriding AISI 316L Austenitic Stainless Steel at Various High Temperatures and Different Gas Nitriding Methods

by

Muhammad Hariz Bin Khairuddin
12738

A project dissertation submitted to
Mechanical Engineering Department
Universiti Teknologi PETRONAS
as partial fulfilment of requirements for the
BACHELOR OF ENGINEERING (Hons)
(MECHANICAL ENGINEERING)

Approved By,

_____
AP Dr. Patthi Hussain

UNIVERSITI TEKNOLOGI PETRONAS

TRONOH, PERAK

AUGUST 2013

CERTIFICATION OF ORIGINALITY

This is to certify that I am responsible for the work submitted in this project, that the original work is my own except as specified in the references and my acknowledgement, and that the original work contained herein have not been undertaken or done by unspecified sources or persons.

_____

MUHAMMAD HARIZ BIN KHAIRUDDIN

ACKNOWLEGDEMENTS

By the Name of Allah, the Most Gracious and the Most Merciful, I would like to express my deepest sense of gratitude to my supervisor, AP Dr. Patthi Hussain for his patient guidance, encouragement, understanding, and excellent advice throughout this project.

I am also in deeply and forever indebted to Mr Askar Triwiyanto, Mr Hassan Mahmoud, Mr Yassar and Mr Syuaib for the time spent on assisting me. Without them, the project will be impossible for me to complete within the time frame.

To the person who inspires me to live my life, who encourage me to put my best efforts, and who believe in me when no one else does. I dedicate this study to my father, Khairuddin Hashim and my beloved mother, Zurinah Mohd Yusof.

Last but not least, I wish to avail myself of this opportunity to express a sense of gratitude to ALL parties who had contributed directly or indirectly to the completion of my project. A warmth gratitude for everyone and may all the goodness will be blessed by Allah.

Thank you.

ABSTRACT

This work investigated the effect of high temperature gas nitriding on AISI 316L to its physical and mechanical properties. In order to modify the surface properties of this material, the samples were treated through gas nitriding at a high temperature of 900˚C hybrid treatment, 1000°C hybrid treatment and 1000°C conventional nitriding method using only nitrogen gas during the heat treatment. These processes have been carried out in a quartz tube furnace for 8hours. The nitrogen, ammonia and methane gases react with the stainless steel to form nitride-layer at its surface. The nitriding results then were analyzed using optical microscopy (OM), Vicker hardness tester, field emission scanning electron microscopy (FESEM), energy dispersive X-ray (EDX) and X-ray diffraction (XRD). From the study, it is found that the surface hardness of the nitrided AISI 316L Austenitic Stainless Steel had increased significantly when compared to the unnitrided sample. The hybrid treatment method also was found out to be far better than the conventional nitriding method, where it greatly increased the diffusivity of the nitrogen, thus producing high properties of nitrided layer results.

Table of Contents

LIST OF FIGURES

LIST OF TABLES

ABBREVIATION AND NOMENCLATURES

ASS = Austenitic Stainless Steel

AISI = American Iron and Steel Institute

EDM = Electrical Discharge Machine

OM = Optical Microscopy

SEM = Scanning Electron Microscope

FESEM = Field Emission Scanning Electron Microscope

XRD = X-Ray Diffraction

EDX = Energy Dispersive X-ray

EDAX = Enery Dispersive X-ray Analysis

FCC = Face Centred Cubic

CHAPTER 1

INTRODUCTION

1.1 Background

Austenitic Stainless Steels (ASS) have been the most common type of stainless steel used nowadays. It has been widely used in many sectors like chemical plant, food processing, architecture, medical appliances and Oil & Gas. ASS is well known for its ductility, ease of working and good corrosion resistance.

ASS is most easily recognized as nonmagnetic. This characteristic made ASS popular in industrial uses especially electronic industry. ASS has an austenitic structure, Face Centred Cubic (FCC) which makes it very ductile and can easily be drawn into thin tubing [1]. While, the reduction of carbon content in many of ASS grades help to improve the weld-able of the ASS, thus it becomes applicable to the applications that need welding joints.

In general, ASS contains elements such as manganese, nickel and molybdenum with 16% to 25 % chromium [2]. Nickel content in ASS is commonly less than 35%. These elements have atomic size that relatively quite large which provides space for smaller atoms like nitrogen and carbon to slips interstitial.

1.2 Problem Statement

In several industries such as electronics and bio-medic, Austenitic Stainless Steel has always been the preferred material to be used in various applications. Yet, there are certain conditions where the surface properties of ASS need to be enhanced for better performance and a wider range of applications. Mechanical properties of ASS such as surface hardness and wear resistance are in need of further improvement and greater enhancement, in order to catch up and be in line with the ever changing demands of today's society.

1.3 Objectives of Study

The study is done to achieve certain objectives:

1. To investigate the physical and mechanical effect of the gas nitriding on AISI 316L ASS at various high temperatures.
2. To compare the effect of different gas nitriding methods on the nitrogen diffusivity.

1.4 Scope of Study

In this research, gas nitriding was performed on raw AISI 316L ASS at 3 different conditions; 900˚C hybrid nitriding, 1000˚C hybrid nitriding and 1000˚C conventional nitriding. Treated samples and raw AISI 316L ASS were then analyzed to investigate their microstructure and hardness. Investigation were carried out using optical microscopy (OM), micro hardness test, field emission scanning electron microscope (FESEM) attached with energy dispersive X-ray (EDX) and X-ray diffraction (XRD).

CHAPTER 2

LITERATURE REVIEW

There are several literatures found related with author's project about the high temperature gas nitriding of Austenitic Stainless Steel. A few of the examples are regarding the characteristics of mechanical properties and microstructure for 316L Austenitic Stainless Steel, development of nitride-layer of AISI 304 Austenitic Stainless Steel during high temperature ammonia gas-nitriding, increasing surface hardness of Austenitic Stainless Steels by pack nitriding process and effect of partial solution nitriding on mechanical properties and corrosion resistance in a type 316L austenitic stainless steel plate.

2.1 Characteristics of Mechanical Properties and Microstructure for 316L Austenitic Stainless Steel

There is a study done on the characteristics of mechanical properties and microstructure for 316L Austenitic Stainless Steel (ASS). In the study, several characteristics of AISI 316L have been discovered [3]. Some of the notable founding are, solution treated AISI 316L found to has better combination strength and elongation than the hot rolled AISI 316L, AISI 316L ASS is easy to work-hardening during deformation, and twins in AISI 316L ASS can be divided into two patterns: suspended twin and transgranular twin. In their study, all samples were cut from hot rolled plate and a few of these samples were taken to be subjected to solution treatment at 1050˚C for 6 minutes. Then, both of the solution treated specimens and hot rolled specimens gone through hardness and tensile tests to evaluate their mechanical properties. Figure 2.1.1 shows the engineering stress vs engineering strain of solution treated specimen and hot rolled specimen.

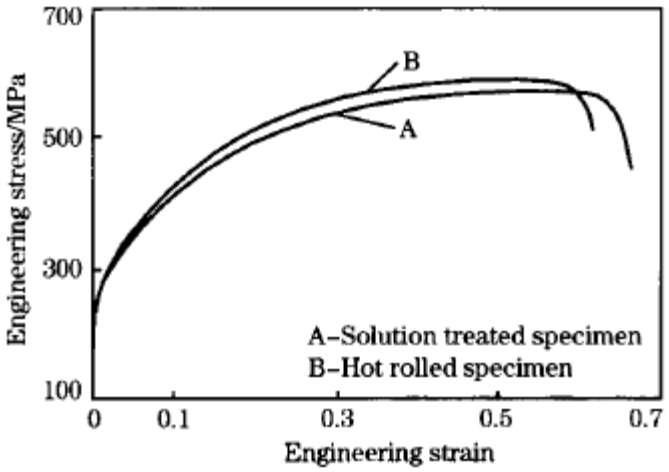

Figure 2.1.1: The engineering stress vs engineering strain graph of solution treated specimen and hot rolled specimen [3]

From the study, it has found out that the solution treated specimen lower the tensile strength from 585MPa to 565MPa, yield strength from 245MPa to 220MPa and hardness from HRB 75.8 to HRB 73.2. Yet, solution treated specimen has better elongation compared to hot rolled specimen from 61.2% to 64.5%. This shows that the solution treated specimen has better combination of strength and elongation.

True stress vs true strain curves and work hardening rate vs true strain are shown in Figure 2.1.2.

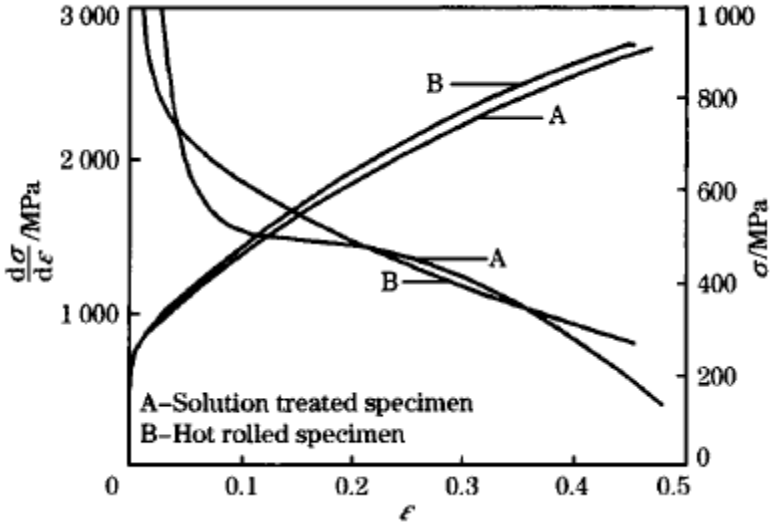

Figure 2.1.2: True stress vs true strain and work hardening rate vs true strain of solution treated specimen and hot rolled specimen

From the work hardening rate vs true strain curves, it is shows that work hardening rate for both specimens decrease gradually with the true strain growing, but overall, solution treated specimen shows a slower decreasing rate. In this study, suspended twin and transgranular twin are also found in scanning electron microscope(SEM) micrographs. Twin growth is feature to the migration of incoherent twin plane and high angle grain boundary rather than the coherent twin plane due to lower energy of coherent twin plane and difficult to migrate. Figure 2.1.3 and figure 2.1.4 shows the suspended twin and transgranular twin respectively in AISI 316L ASS.

Figure 2.1.3: Suspended twin observed using SEM

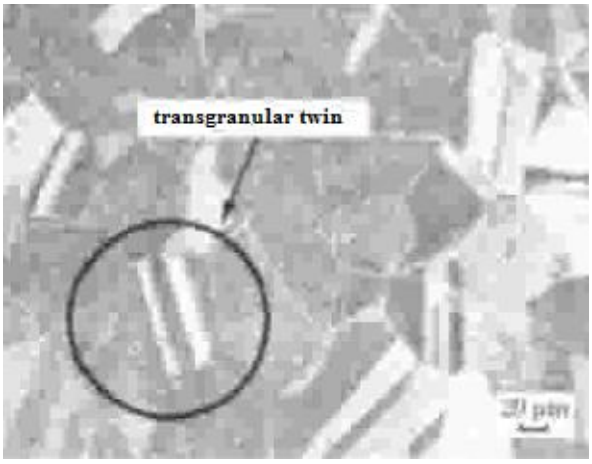

Figure 2.1.4: Transgranular twin observed using SEM

2.2 Development of Nitride-layer of AISI 304 Austenitic Stainless Steel during High Temperature Ammonia Gas-Nitriding

Peng et. al [4] have checked out on the development of nitride-layer of Austenitic Stainless Steel(ASS) from high temperature gas nitriding. The experiment showed 4 unique sub-layer composed in the nitride-layer formed, which are CrN (particles) + Fe_4N (+Cr_2N), S (or S + CrN), ɣ+ CrN (fine lamellar + particles), and ɣ +Cr_2N (coarse lamellar). In the study, nitriding process was done in a quartz tube, where samples are exposed with pure ammonia gas in high temperature. Tests are repeated with variation of high temperatures at 860°C and 1020°C for a period of 6 hours. Figure 2.2.1 shows optical micrograph of nitrided specimen at 1020°C.

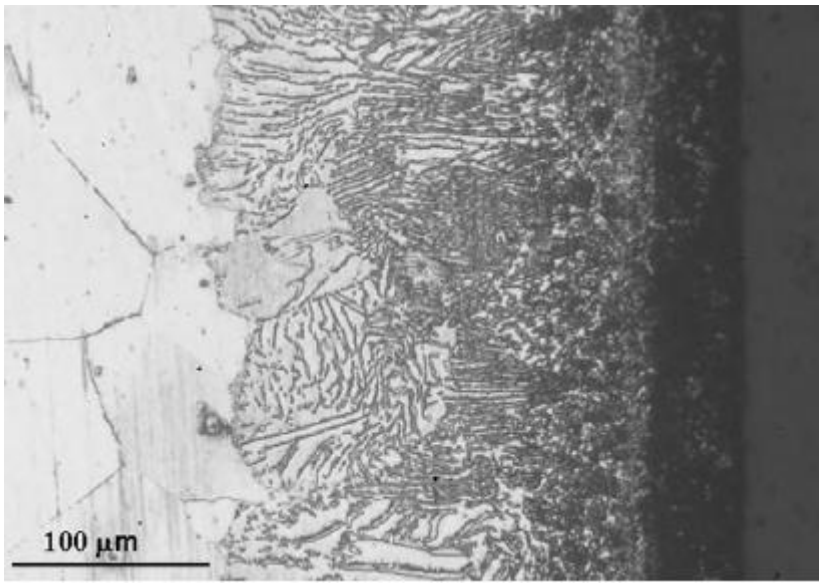

Figure 2.21: Optical Micrograph of nitrided specimen at 1020˚C [4]

From the optical micrograph above, it is clearly noted that the nitride-layer appeared to be consisted of four layers.

Figure 2.2.2 and 2.2.3 show SEM micrographs of nitride-layers composed of four sub-layers, which was developed at 1020°C and 860°C respectively.

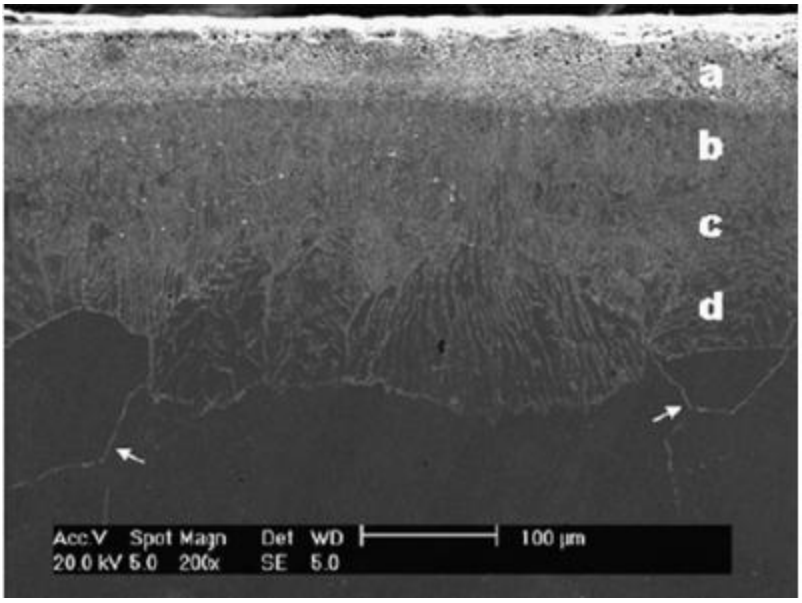

Figure 2.2.2: SEM micrograph of a nitride-layer composed of four sub-layers, which was developed at 1020 ◦C

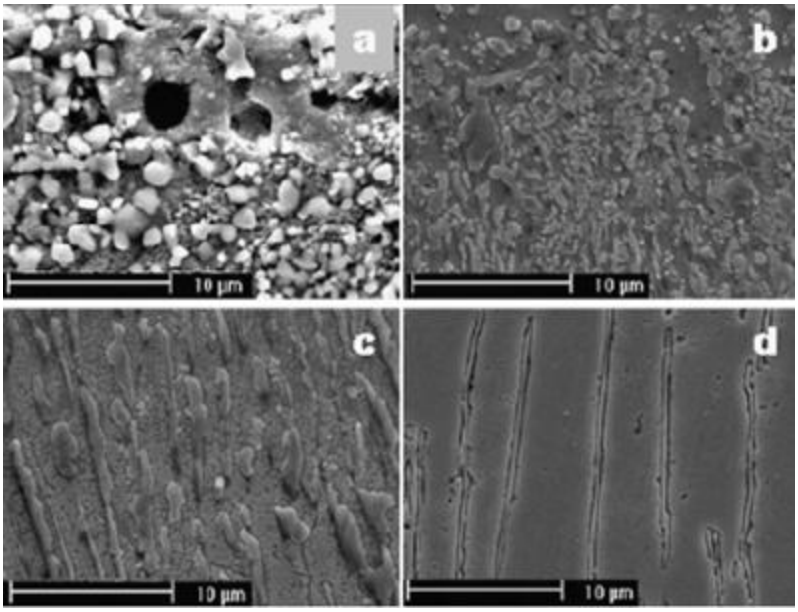

Figure 2.2.3: SEM micrographs of a nitride-layer composed of four sub-layers, which was developed at 1020 ◦C; enlarged images of each sub-layer (a: first; b: second; c: third; d: fourth sub-layer).

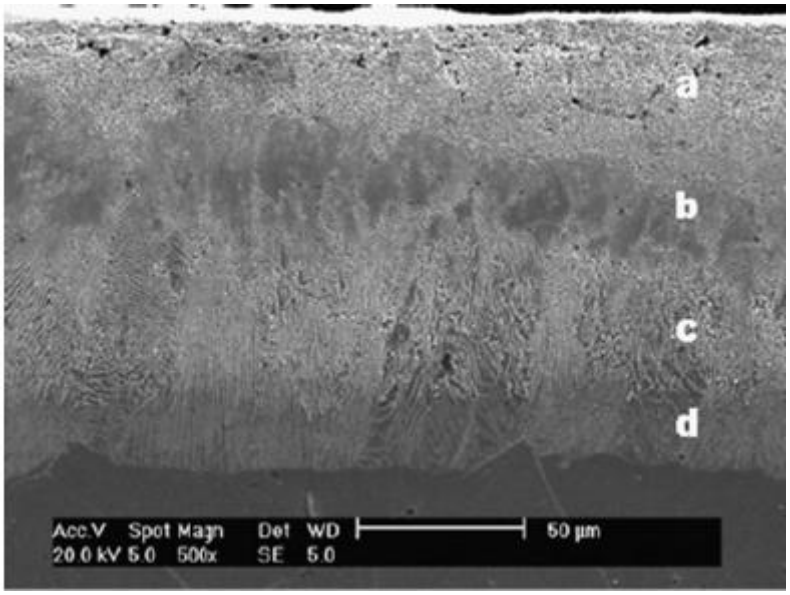

Fig. 2.2.4: SEM micrograph of a nitride-layer composed of four sub-layers, which was developed at 860 ◦C

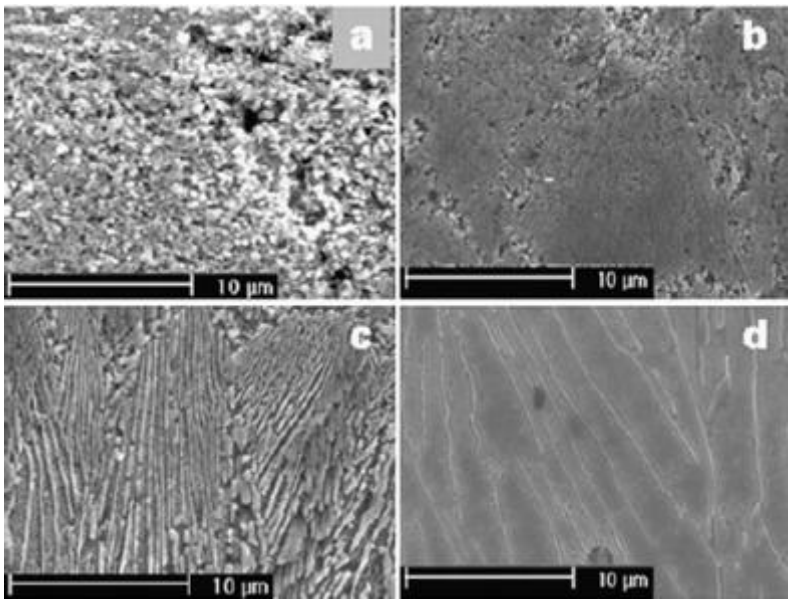

Fig. 2.2.5: SEM micrographs of a nitride-layer composed of four sub-layers, which was developed at 860 ◦C; enlarged images of each sub-layer (a: first; b: second; c: third; d: fourth sub-layer). [4]

SEM equipped with EDAX was used to get a better characterization of the samples microstructure. An overall picture of nitride-layer developed at 1020°C showed that it was consisted of four sub-layers. From the first sub-layer, we can see a mixture of bulky aggregates (near surface) and dense round particles. Micro-cracks and pores were often observed in this sub-layer. The second sub-layer was not too distinctively

recognizable at this temperature, as it appeared to be composed of degenerated bulky aggregates. The third sub-layer displayed a short lamellar structure intermixed with round particles. The fourth sub-layer showed a typical coarse lamellar structure.

The four sub-layers of the nitride-layer was much more distinctive in the SEM image of the specimen nitrided at 860 °C. The first sub-layer appeared to be a porous structure, which consists of fine particles and aggregates. The second sub-layer composed of bulk-like structure occasionally embedded with fine particles and it was clearly distinguishable from the first sub-layer. A fine and dense lamellar structure composed with fine particles are shown in the third sub-layer. The fourth sub-layer displayed a coarse lamellar structure.

2.3 Increasing Surface Hardness of Austenitic Stainless Steels by Pack Nitriding Process

Previous work shows that by increasing nitrogen content through high temperature nitriding, will improve the surface hardness as well as wear resistance of Austenitic Stainless Steel [5]. In the study, K.Y. Li and X. D. Ziang pick pack nitriding method in order to nitride the Austenitic Stainless Steel. Cr_2N powder was used as the source of nitrogen, since partial pressure generated in the pack is very low. Figure 2.3.1 shows how temperature may effect greatly on the dissocation pressure. It can be seen that nitrogen pressure in the pack change drastically from 4 Pa at 860°C to 5539 Pa at 1200˚C. Therefore, they decide to take variation in temperatures of pack nitriding, in order to result in different outcomes. Two nitriding tempereatures were taken; which are 860˚C and 920˚C, with AISI 304 ASS samples are used as the testing material.

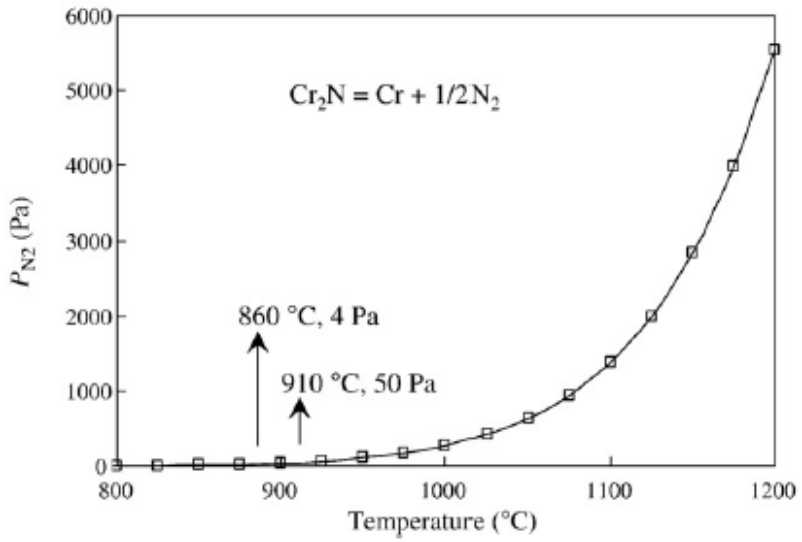

Figure 2.3.1: Nitrogen dissociation pressure of Cr_2N against temperature. [5]

To analyse the surface hardness of the AISI 304 ASS after nitriding, samples were undergone micro hardness testing. Figure 2.3.2 and 2.3.3 show the result of the micro hardness test.

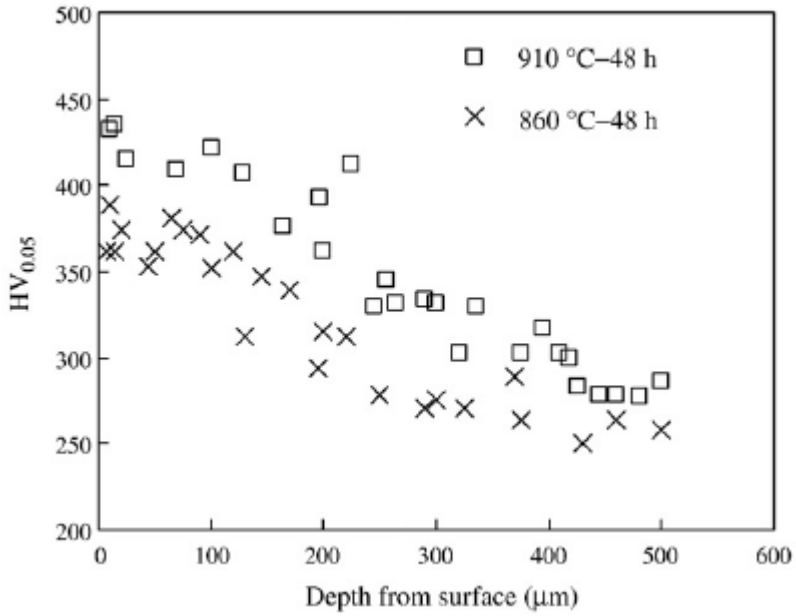

Figure 2.3.2: Effect of pack nitriding temperature on the microhardness profile.

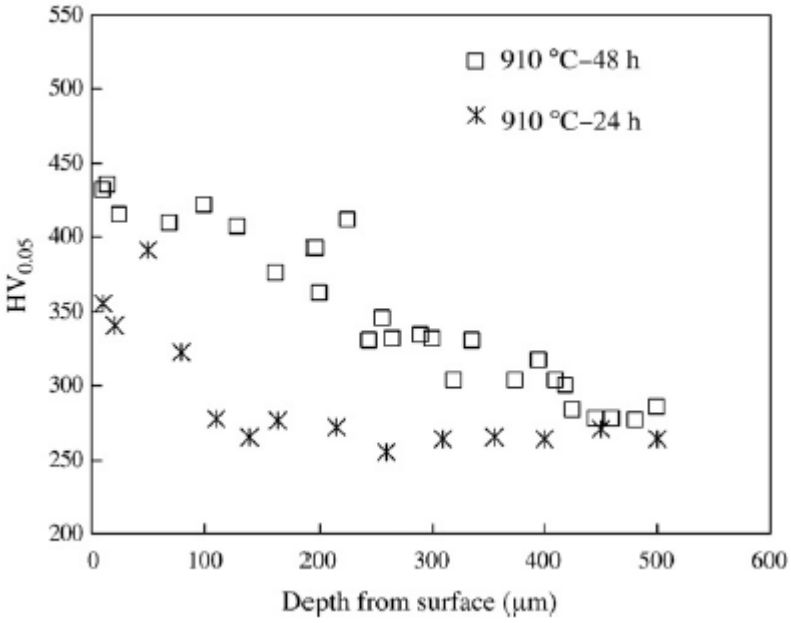

Figure 2.3.3: Effect of time on the microhardness profile for specimens nitrided at 910 °C.

Figure 2.3.2 compares the microhardness for the specimen nitrided at 860˚C and specimen nitrided at 910˚C. From the figure, it clearly shows that as time nitriding time increases, both of the specimens increase in their surface hardness. At the same time, compared time to time, nitrided specimen at a higher temperature of 910˚C apparently has better surface hardness compared to the nitrided specimen at 860˚C. While figure 2.3.2 is comparing specimens of different nitriding temperature, figure 2.3.3 show the difference of micro hardness profile for the same sample, which nitrided at 910˚C but with the different of nitriding time. From the figure, it is clearly notable that a longer nitriding duration, will caused a better wear resistance of the sample. As a conclusion, both of these analysis shows that nitriding may far improve the wear resistance of an ASS. Higher in nitriding temperature means higher nitrogen partial pressures and also higher nitrogen diffusion rate. Longer duration means better nitrogen diffusion on the sample surface. Thus, from this study, it is apparent that nitriding improves the surface hardness and wear resistance of ASS.

2.4 Effect of Partial Solution Nitriding on Mechanical Properties and Corrosion Resistance in a Type 316L Austenitic Stainless Steel Plate

T. Nakanishi et. al [6] points out that solution nitriding may improved the properties of the Austenitic Stainless Steel used as commercial osteosysnthesis implants and to also reduce the plate thickness. The solution nitriding time varied up to 10 hours, which effect the nitrogen concentration distribution in the steel plates, AISI 316L ASS. Nitriding works are done using the exposure of N_2 gas at a high temperature of 1473K. The material properties are examined to show the effect of unsaturated(partial) solution nitriding.

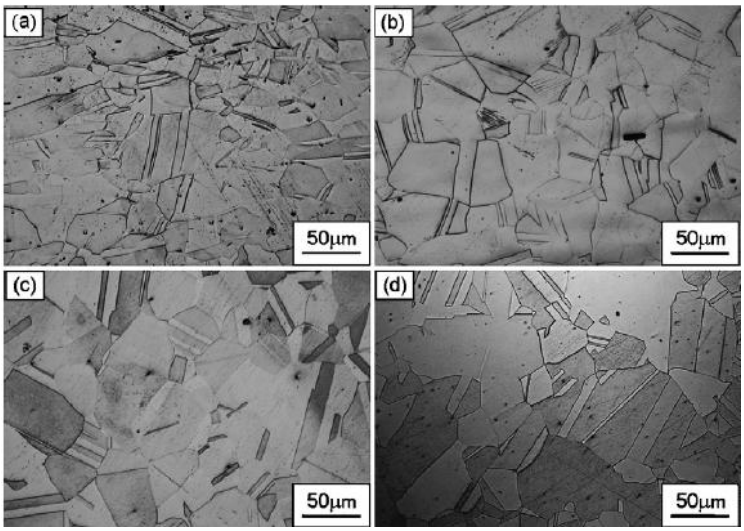

Figure 2.4.1: Optical micrographs of the nitrogen-free 316L austenitic steel (a) and solution-nitrided 316L ones (b–d) [6].

Figure 2.4.1 above shows the optical micrographs of AISI 316L ASS solution nitrided for 0ks (a), 0.6ks (b), 4.8ks (c) and 36ks (d). It is apparent that the grain size of austeinitic tends to grow larger as solution nitriding time increases.

Figure 2.4.2 below shows the vicker hardness profiles of the AISI 316L steel solution nitrided samples. The original hardness level (without solution nitriding) is indicated by the broken line, which is 1.7Gpa. From comparing the curves, we can easily noted that the longer duration of solution nitriding gives better surface hardness to the steel. This same characterisics are consistent with K.Y. Li and Z.D. Xiang results [5].

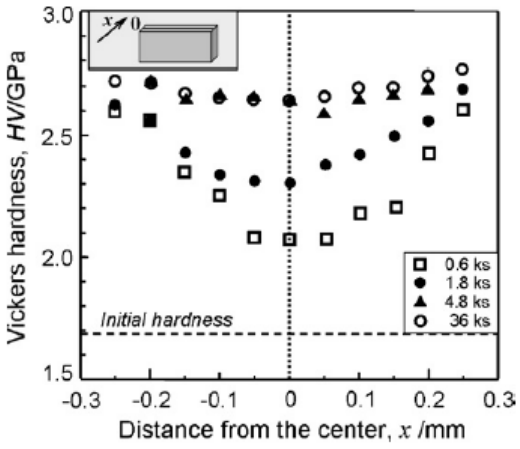

Figure 2.4.2: Vickers hardness profiles of the 316L steel solution-nitrided for 0.6, 1.8, 4.8, and 36 ks [6].

In Nakashi et. al study, corrosion behaviour of the samples are also investigated to observed the effect of partial nitriding to the corrosion resistance of AISI 316L [6]. Figure 2.4.3 shows anodic polarization curves measured in 1M NaCl solution at 298K (room temperature) in the nitrogen-free 316L and the solution nitrided one. From the curves, it clearly shown that nitrided samples has better corrosion resistance that nitrogen free sample. However, 1.8ks partial nitriding time is sufficient in obtaining quality corrosion resistance surface, since it has corrosion resistance equal to fully solution nitrided steel in this case.

As the conclusion, high temperature nitriding helps in improving wear resistance and surface hardness of ASS and these has been proven in many studies. The analysis of nitrided samples at high temperatures and varying nitriding methods are still lacking, and here come the urge to highlight and study further on the issue, in order to find the best nitriding method and condition to yield the best physical and mechanical properties of ASS.

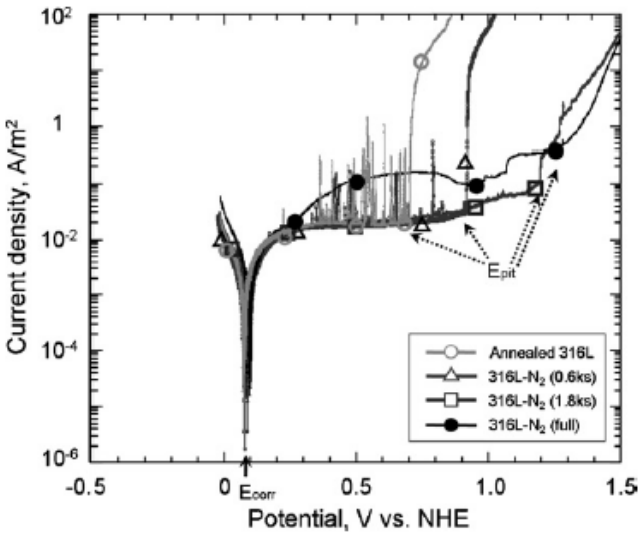

Figure 2.4.3: Anodic polarization curves measured in 1M NaCl solution at 298K (room temperature) in the nitrogen-free 316L specimen, and the solution-nitrided specimens. The solution nitriding were performed for 0.6, 1.8, and 4.8 ks [6].

CHAPTER 3

METHODOLOGY

3.1 Project Flow

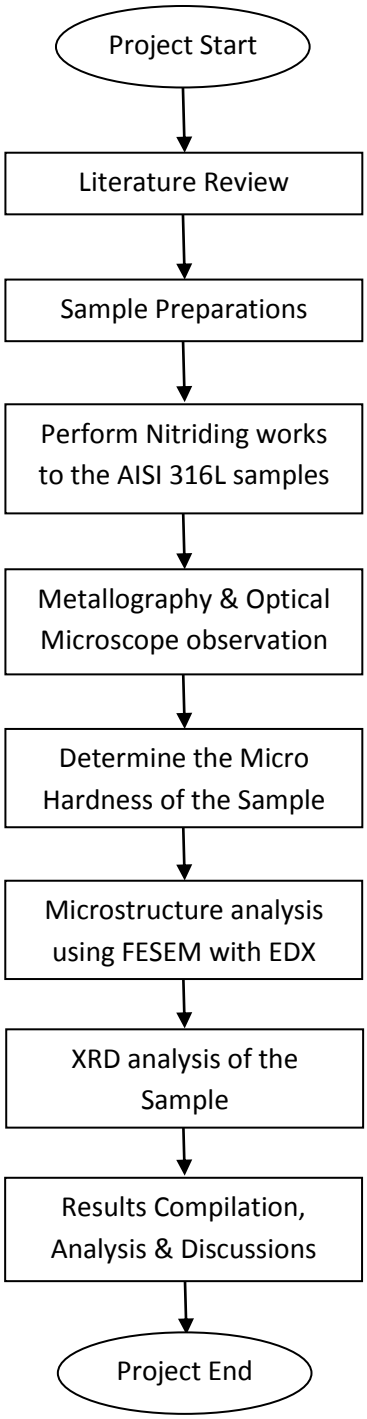

Figure 3.1: Methodology of the project

3.2 Gantt Chart

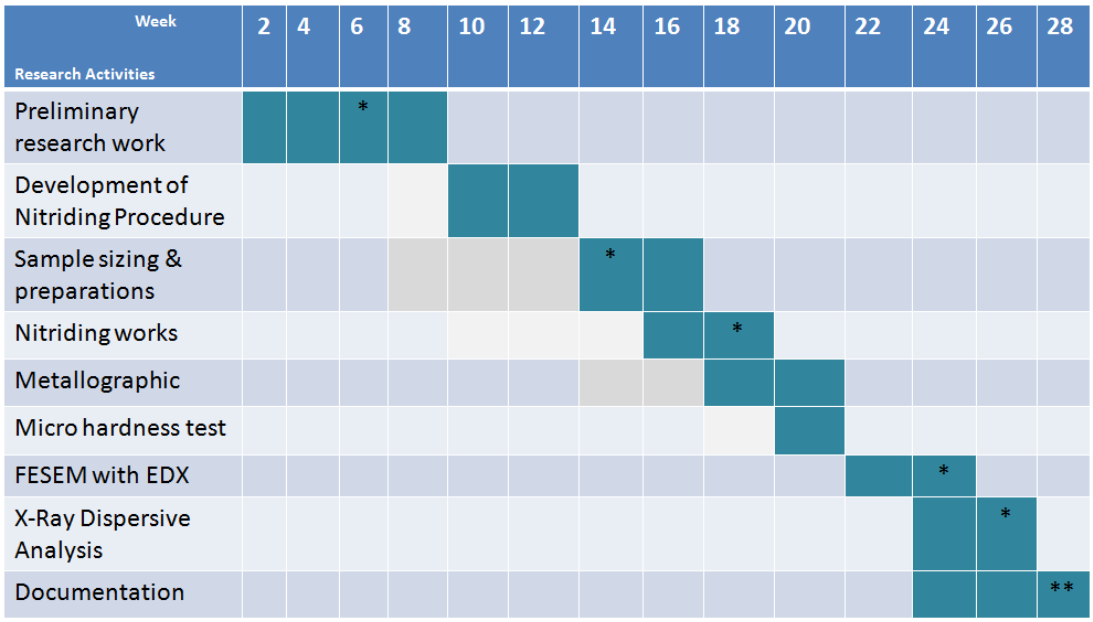

Figure 3.2: Research's Gantt chart

*Key milestones

Week 6: Submission of Extended Proposal

Week 14: Submission of Interim Report

Week 18: Completion of nitriding works

Week 25: Pre-SEDEX

Week 27: Completion of all test and analysis works

Week 28: Submission of Dissertation

Week 28: Submission of paper for the 22nd Scientific Conference of Microscopy Society Malaysia (MSM 2013)

3.3 Nitriding Experiment

The experiment started with 1000˚C hybrid nitriding which is known as preliminary experiment before proceeding with hybrid 900˚C and conventional 1000˚C. After that, several tests are carried out in order to analyze the effect of nitriding to the samples. The experiment was conducted successfully. Some important parameters are set before the experiment. For the hybrid nitriding works, we used 3 types of gases, which are nitrogen, ammonia and methane with the composition set at a ratio of 75:20:5. While for the conventional nitriding, only nitrogen gas was used during the experiment. The heat treatment time used for all the experiments is 8hours with 10˚C/min ramping rate. The samples prepared were arranged in the Alumina boat. The boat was then pushed by a long stick to ensure the samples were placed in the middle of the furnace. Every step was needed to be followed properly and personal protection equipment must be worn while performing the experiment.

The procedure of the nitriding experiment is as follow;

<u>At the beginning</u>

1. Samples were immersed in hydrochloric acid for about 15-30 minutes.
2. The cover of the tube furnace was opened.
3. The samples were arranged in the alumina bot.
4. Alumina boat was pushed into the middle of the quartz tube.
5. The furnace cover was closed.
6. Nitrogen gas valve was opened.
7. Air was purged in the furnace for about 15 minutes using nitrogen gas
8. The instruction on the controller was set and followed.

<u>Heat treatment</u>

1. Ammonia gas valve was opened (only for hybrid treatment).
2. Methane gas valve was opened (only for hybrid treatment).
3. Gas flows are regulated to the desired flow rate at respective regulators. (Nitrogen at 140ml/min, ammonia at 50ml/min, methane at 10ml/min)

Cooling down

1. Ammonia gas valve was closed (only for hybrid treatment).
2. Methane gas valve was closed (only for hybrid treatment).

End

1. Nitrogen gas valve was closed
2. Check all the gas valve (closed position)
3. Ensure temperature of the furnace is below 100˚C before tube furnace was opened
4. Samples were taken out
5. Switch off power (furnace)

Figure 3.3.1: Preparing equipment and appliances setup for nitriding work

Figure 3.3.2: Sample preparation by immersing samples to be nitrided into hydrochloric acid

Figure 3.3.3: Pushing alumina boat using long stick before the experiment start

Figure 3.3.4: Tube furnace during heating process (noted that the temperatures shown at the temperature indicators are almost 900°C – first heat treatment temperature)

Figure 3.3.5: Samples after nitrided and its position arrangement in alumina boat

3.4 Metallographic

Metallography is the science and art of preparing a metal surface for analysis by grinding, polishing, and etching to reveal microstructual constituents. After preparation, the sample can easily be analyzed using optical or electron microscopy.

3.4.1 Sectioning

After the samples were received, they were cut into required sizes. The objective is to prepare for tests other than microstructure or macrostructure structure. The tool that author used to cut the specimen is abrasive cutter. Abrasive cutting is the sectioning of material using a relatively thin rotating disk composed of abrasive particles supported by a suitable medium. Each sample was cut to same size which is 15mm x 10mm x 1.5mm.

3.4.2 Mounting

Metallographic specimens were cut to an appropriate size, mounting of the specimen is often desirable or necessary for subsequent handling and metallographic polishing. The specimen was placed in the mounting press, the resin was added, and the sample was processed under heat and high pressure. The pressure used to mount the resin was set to 1200psi. Time allocated for the heat time was about 2 minutes and for the cooling time was about 3 minutes. The machine used to mount the sample is Simplimet Auto Mounting Press.

Figure 3.4.2: Mounted samples

3.4.2 Grinding

Investigations continue by grinding the mounted specimen to the parallel surface finish. The abrasive particles are forced into a flat surface of a comparatively soft material. The specimen is successively ground with finer and finer abrasive media. Silicon carbide sandpaper was the first method of grinding and is still used today.

Many metallographers, however, prefer to use a diamond grit suspension which is dosed onto a reusable fabric pad throughout the polishing process. Diamond grit in suspension might start at 9 micrometers and finish at one micrometer. Generally, polishing with diamond suspension gives finer results than using silicon carbide papers (SiC papers), especially with revealing porosity, which silicon carbide paper sometimes "smear" over. Because the austenitic grades work harden readily, cutting and grinding must be carefully executed to minimize deformation. The machine used to grind the sample is METASERV 2000.

Figure 3.4.3: Grinding and polishing machine used (METASERV 2000)

3.4.4 Polishing

After grinding the specimen, polishing was performed. Typically, a specimen was polished with slurry of alumina, silica, or diamond on a napless cloth to produce a scratch-free mirror finish, free from smear, drag, or pull-outs and with minimal deformation remaining from the preparation process.

3.4.5 Etching

After polishing the sample, microstructural constituents of the specimen were revealed by using a suitable chemical or electrolytic etchant. A great many etchants have been developed to reveal the structure of metals and alloys, ceramics, carbides, nitrides, and so forth. While a number of etchants may work for a given metal or alloy, they generally produce different results, in that some etchants may reveal the general structure, while others may be selective to certain phases or constituents. The

etchants that author used for the austenitic stainless steel are Glyceregia. Author had chosen the best etchant which is Glyceregia's reagent, the ingredient for this particular etchant are;

45ml Glycerol.
15ml Nitric Acid
30ml Hydrochloric Acid

The procedure of etching;

a) Specimen was cleaned by the distilled water.

b) Next, specimen was dip with the alcohol to remove the dirt and contamination.

c) Then, the specimen was swabbed with the etchant.

d) After 5minutes the specimen was rinsed with distilled water.

e) Again, the specimen was dip in the Ethanol.

f) Finally, the specimen was dried by using the dryer.

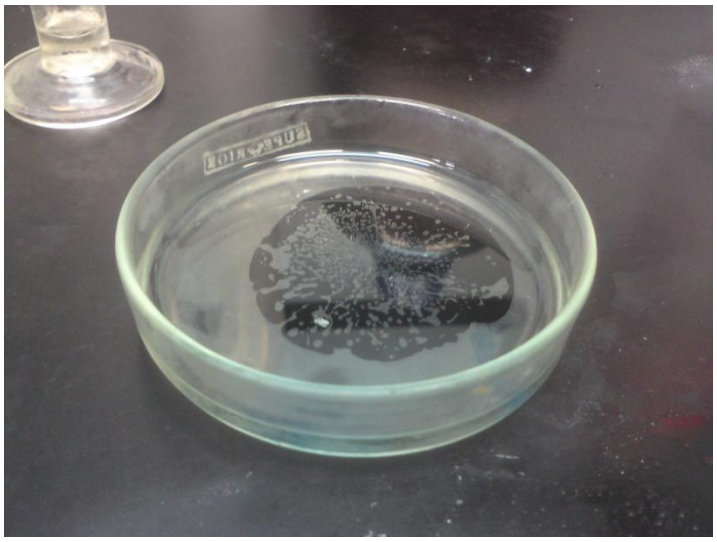

Figure 3.4.5: Glyceragia in dipping dish for sample dipping

3.4.6 Light Microscopy

Light optical microscopy remains the most basic tool for the study of microstructure. At first the magnification start with low magnification, such as 5x, followed by progressively higher magnification for efficient assessment of the basic characteristic of the microstructure.

Figure 3.4.6: LEICA optical microscope used for optical microscopy (OM)

3.5 Vickers Hardness Testing

Vickers Hardness tester was used to measure the hardness of the sample. The basic principle, as with all common measures of hardness, is to observe the questioned materials' ability to resist plastic deformation from a standard source. The Vickers Hardness test can be used for all metals and has one of the widest scales among hardness tests. For the hardness tests on the samples, test load is set at 25gf and 10seconds dwelling time. The machine used to perform the hardness test was micro hardness tester Model LECO LM247 AT.

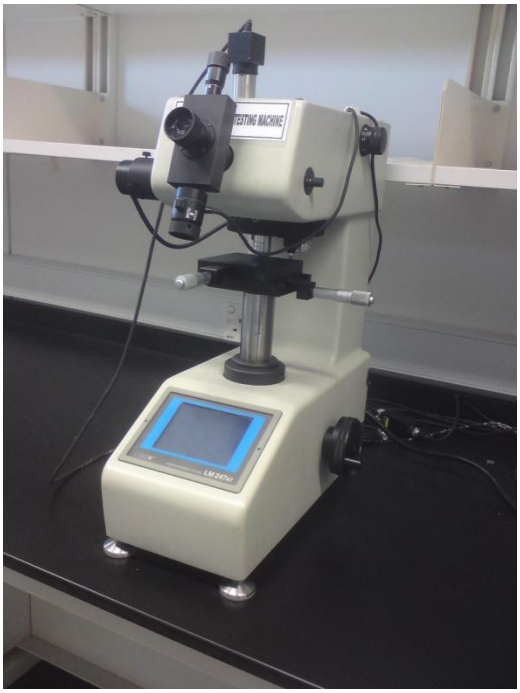

Figure 3.5: LECO LM247 AT micro hardness tester

CHAPTER 4

RESULTS AND DISCUSSION

4.1 Effect of nitriding to AISI 316L ASS at various high temperature

Figure 4.1.1 shows the microstructure of hybrid nitrided sample at 900°C at 200x magnification rate. From the surface going down deeper into the sample, different form of microstructure can be seen due to different sub-layers formed from the hybrid nitriding process. To analyze in greater details, the microstructure was analyzed separately into 4 distinguish sub-layers, let it be initial as a, b, c and d.

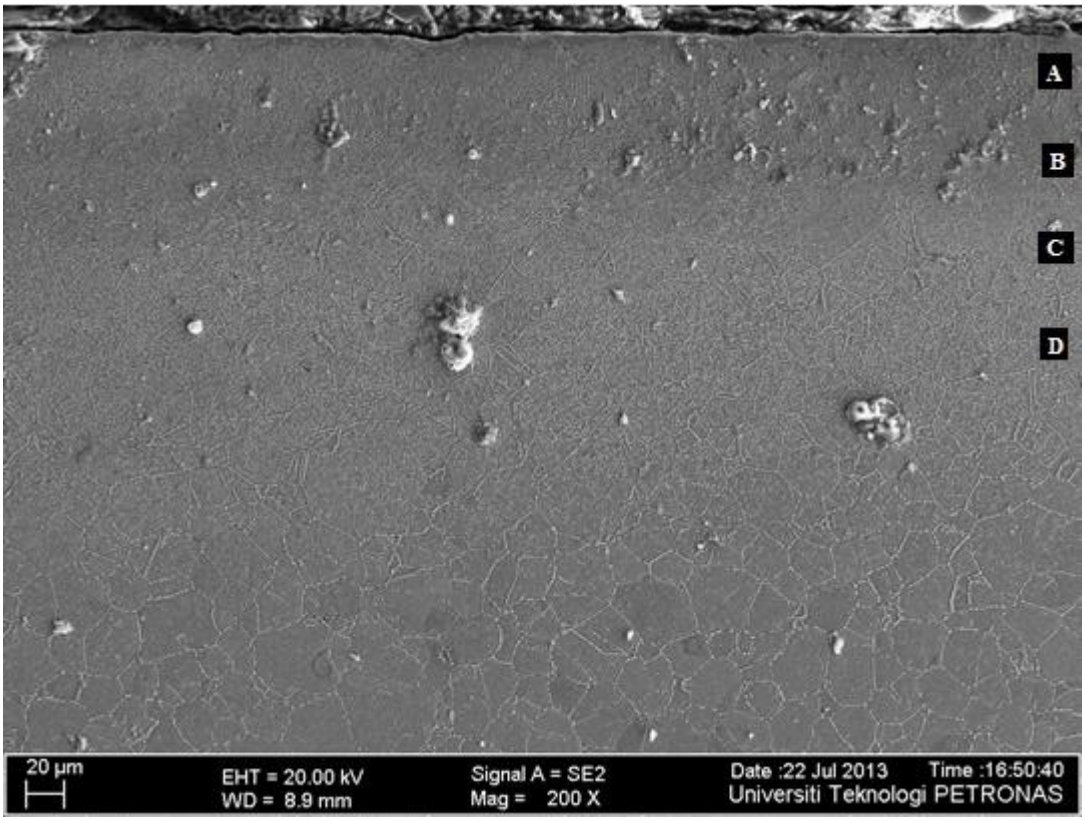

Figure 4.1.1: Microstructure of hybrid nitrided sample at 900°C using FESEM

Figure 4.1.2A, we can see the first sub-layer formed which is the layer closest to the surface sample. Fine and densed lamellar structure associate with fine particles was formed at the layer. At the second sub-layer (Figure 4.1.2B), tiny but densed lamellar structure seen scattered all over the layer with a some twinning elements noted in the layer showing the austenitic characteristic of the layer. The third sub-layer (Figure 4.1.2C) showed a short and densed lamellar structure scattered associated with

twinning elements in grains formations. The fourth sub-layer shown in Figure 4.1.2D is composed with formation of bigger grains associated with fine particles and aggregates. The unique lamellar structure formed throughout the gas diffused zone may be explained by the presence of carbon given by methane.

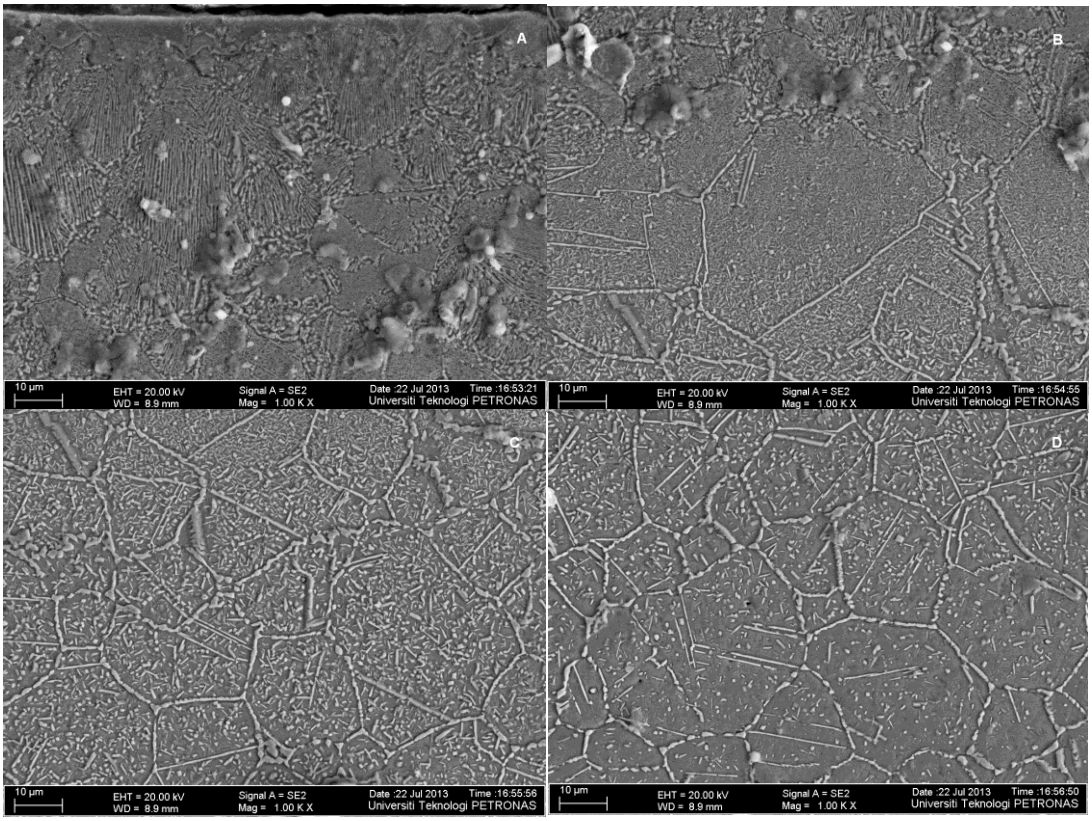

Figure 4.1.2: Microstructure of hybrid nitrided sample at 900°C at different sub-layers; A: first, B: second, C: third, and D: forth

EDX analysis in Table 4.1.1 and Table 4.1.2 show nitrogen and chromium content degraded as we go deeper along the cross-section of the sample. This may results into different sub-layers formed at the sample surface. Microstructure also showed S-phase or expanded austenite phase formed by the nitriding process. The S-phase was known to be formed by incorporation of excess amount of nitrogen into austenite phase and was formed by an expansion of austenite [4]. Therefore, dislocation movement was expected hardly to happen and its hardness was expected to be extremely high.

Element	Weight%	Atomic%
C K	1.59	4.74
N K	7.61	19.50
O K	10.06	22.54
Cr K	33.62	23.19
Mn K	0.95	0.62
Fe K	40.25	25.85
Ni K	5.62	3.43
Mo L	0.30	0.11
Totals	100.00	

Table 4.1.1: EDX analysis of hybrid nitrided sample at 900°C on the first sub-layer

Element	Weight%	Atomic%
C K	-4.65	-22.10
N K	2.10	8.57
O K	3.11	11.09
Cr K	13.79	15.13
Mn K	1.41	1.46
Fe K	76.06	77.74
Ni K	8.58	8.34
Mo L	-0.40	-0.24
Totals	100.00	

Table 4.1.2: EDX analysis of hybrid nitrided sample at 900°C on the second sub-layer

Figure 4.1.3 shows the microstructure given by FESEM of hybrid nitrided sample at temperature of 1000°C at 350x magnification. From the surface going down deeper into the sample, different form of microstructure can be seen due to different sub-layers formed from the hybrid nitriding process. To analyze in greater details, the microstructure will be analyzed separately into 4 distinguish sub-layers, let it be initial as a, b, c and d.

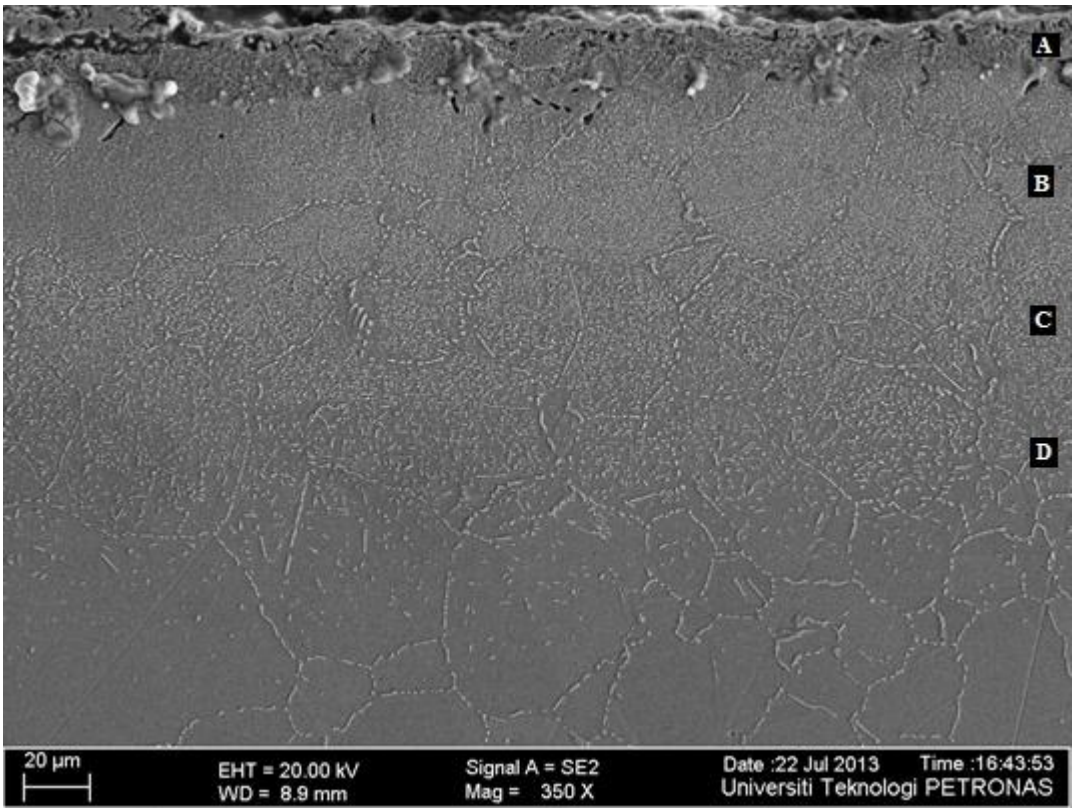

Figure 4.1.3: Microstructure of hybrid nitrided sample at 1000°C using FESEM

Figure 4.1.4A, shows microstructure of the first sub-layer formed which is the layer closest to the surface sample. Porous structure with fine particles and aggregates was observed at the layer. At the second sub-layer (Figure 4.1.4B), short and densed lamellar structure seen scattered all over the place. The third sub-layer in Figure 4.1.4C shown grain formation associated with short lamellar structure. The fourth sub-layer (Figure 4.1.4D) is composed with formation of bigger grains but with no lamellar structure to be found in the grains. The unique lamellar structure formed throughout the gas diffused zone may be explained by the presence of carbon given by methane.

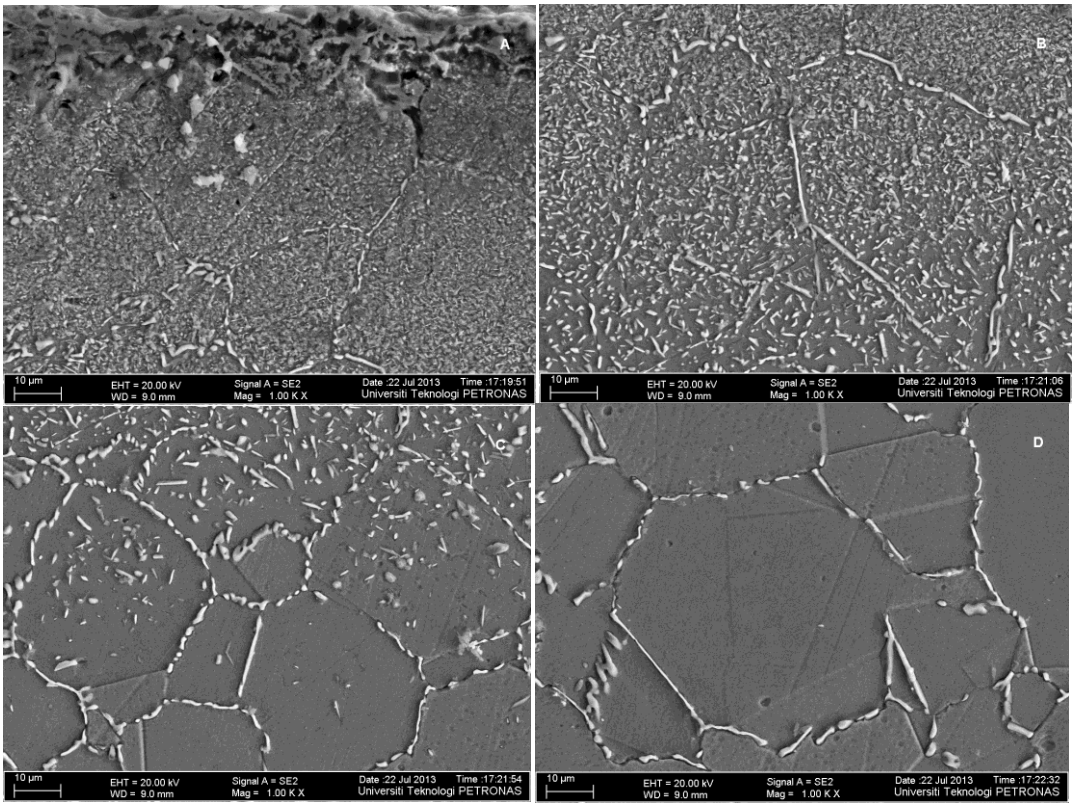

Figure 4.1.4: Microstructure of hybrid nitrided sample at 1000°C at different sub-layers; A: first, B: second, C: third, and D: forth

EDX analysis in Table 4.1.3 and Table 4.1.4, shown similar results with 900°C hybrid nitriding, where chromium content degraded as we go deeper along the cross-section of the sample. This may results into different sub-layers formed at the sample surface. S-phase structure may also be seen showing the by incorporation of nitrogen into the sample change its austenite phase to expanded austenite. Hardness is expected to be very high and dislocation movement expected to be very limited by the formation of the S-phase.

Element	Weight%	Atomic%
C K	9.96	22.38
N K	-2.43	-4.68
O K	30.29	51.12
Cr K	30.76	15.97
Mn K	2.10	1.03
Fe K	29.31	14.17
Totals	100.00	

Table 4.1.3: EDX analysis of hybrid nitrided sample at 1000°C on the first sub-layer

Element	Weight%	Atomic%
C K	-12.28	-65.17
N K	8.47	38.56
O K	2.39	9.52
Cr K	23.54	28.85
Mn K	1.67	1.94
Fe K	68.30	77.96
Ni K	7.30	7.93
Mo L	0.61	0.41
Totals	100.00	

Table 4.1.4: EDX analysis of hybrid nitrided sample at 1000°C on the second sub-layer

The Figure 4.1.5, 4.1.6 and 4.1.7 show the X-Ray diffraction (XRD) analysis of raw AISI 316L sample, 900°C hybrid nitrided sample and 1000°C hybrid nitrided sample respectively. Three highest peaks was highlighted at the XRD raw sample which occur at 43.8 2θ (87.6°), 44.9 2θ (89.8°) and 50.6 2θ (101.2°). From the peak when analyzed using EVA software, it was found that the layer composed hugely by three compounds. They are iron nickel and chromium iron nickel carbon compounds. XRD analysis for 900°C hybrid nitrided sample, two highest peaks was highlighted

which occur at 43.2 2θ (86.4°), and 43.7 2θ (87.4°). Analyzing the peaks, it was found that the layer composed hugely by chromium nitride (Cr_2N), chromium nitride (CrN) and siderazot (Fe_3N). For 1000°C hybrid nitrided sample, two highest peaks highlighted occur at 20.2 2θ (40.4°), and 35.5 2θ (71.0°). Matching the XRD graph in the XRD graph compound database, it was found that the sample composed largely by chromium nitride (Cr_2N), siderazot (Fe_2N) and chromium carbide nitride.

The phase formations of nitrides were obtained from both 900°C hybrid nitrided sample and 1000°C hybrid nitrided sample. From the XRD pattern, it was observed that iron nitrides are formed at the peaks with nitrogen formation. The formation of Cr-Ni-Fe-C elements such as siderozot, iron nitride and chromium carbide nitride in both nitrided samples expected to improve the wear resistance of the material. While the formation of chromium carbide and chromion nitride compounds, shows depletion of chromium thus there is a possibility of degradation of corrosion resistance of the material.

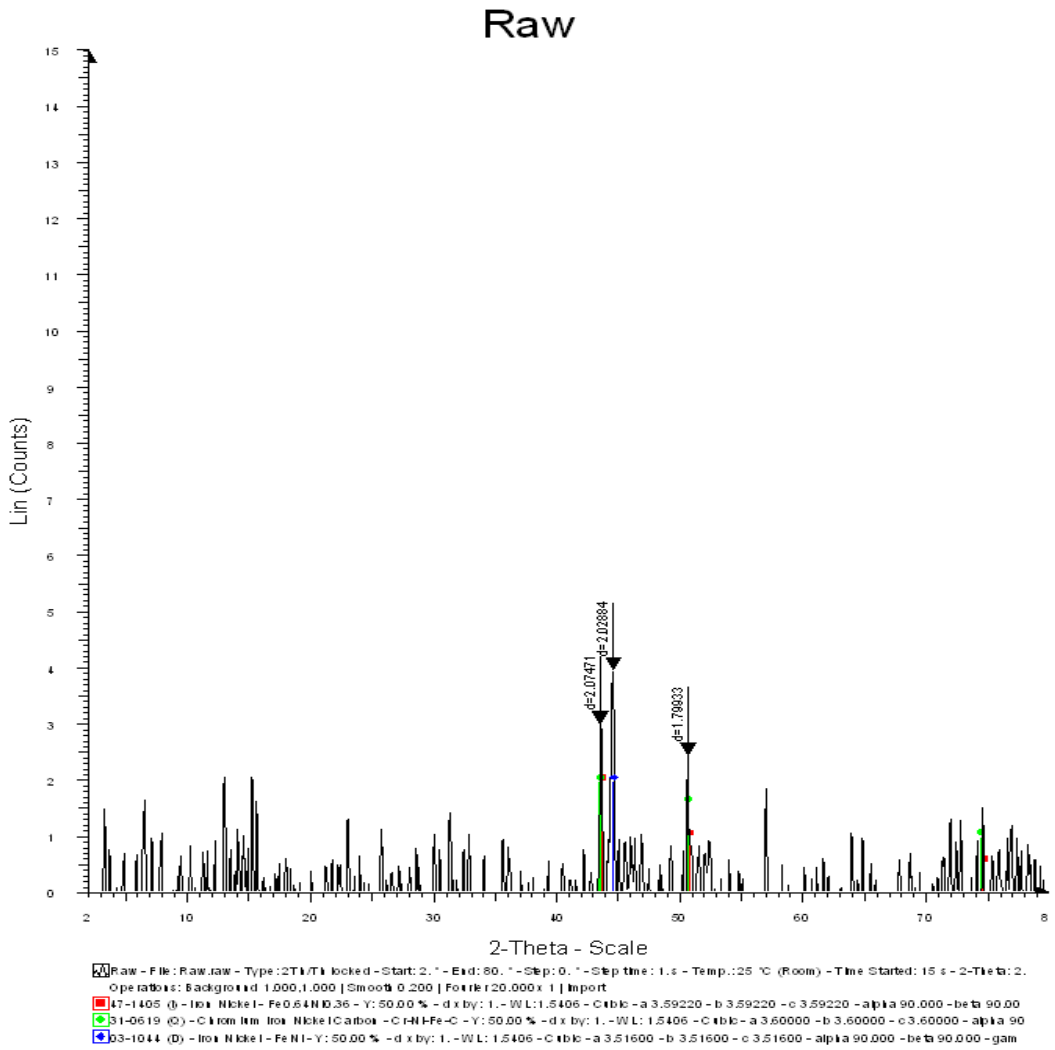

Figure 4.1.5: XRD graph analysis on raw sample

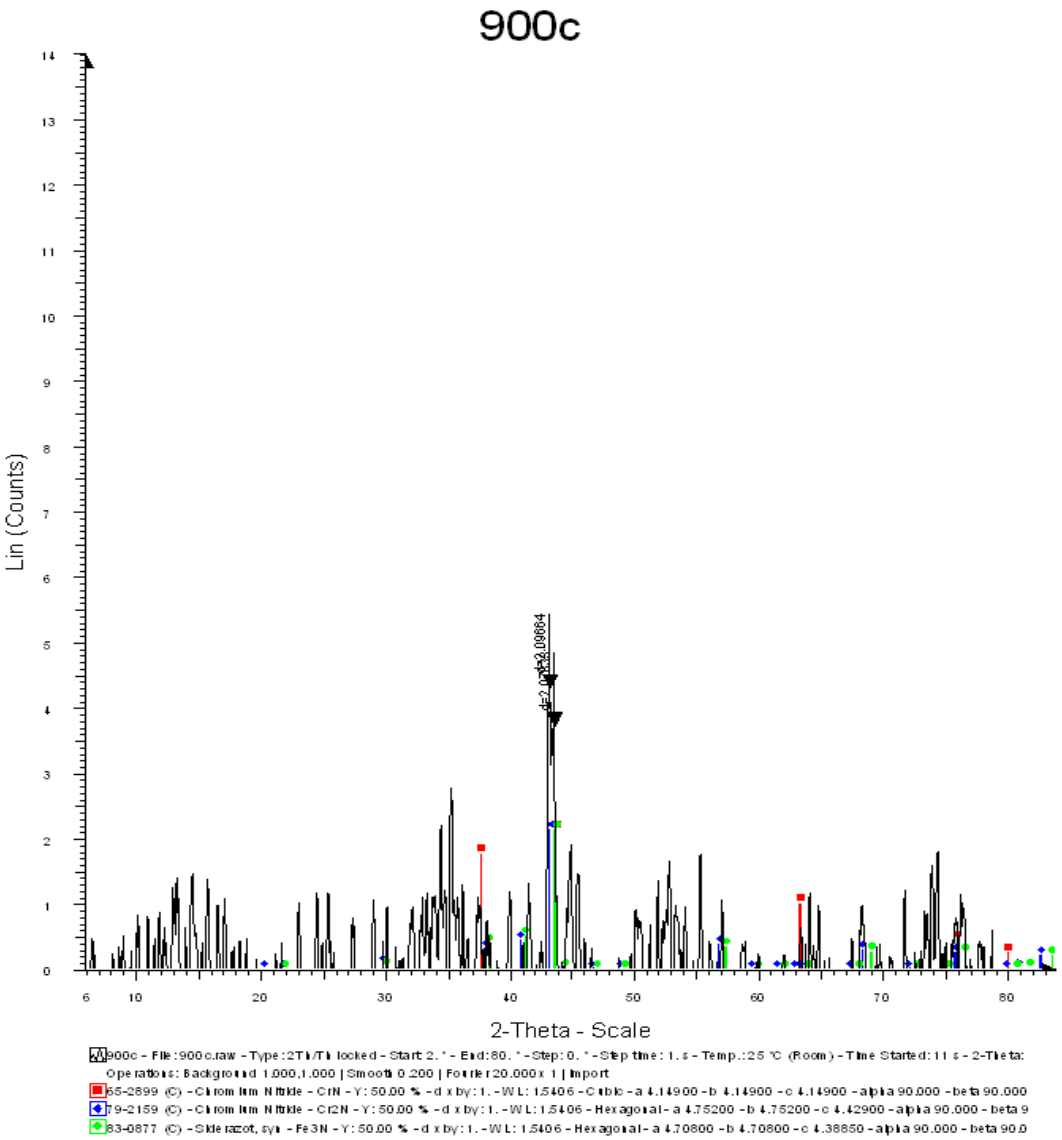

Figure 4.1.6: XRD graph analysis on 900°C hybrid nitrided sample

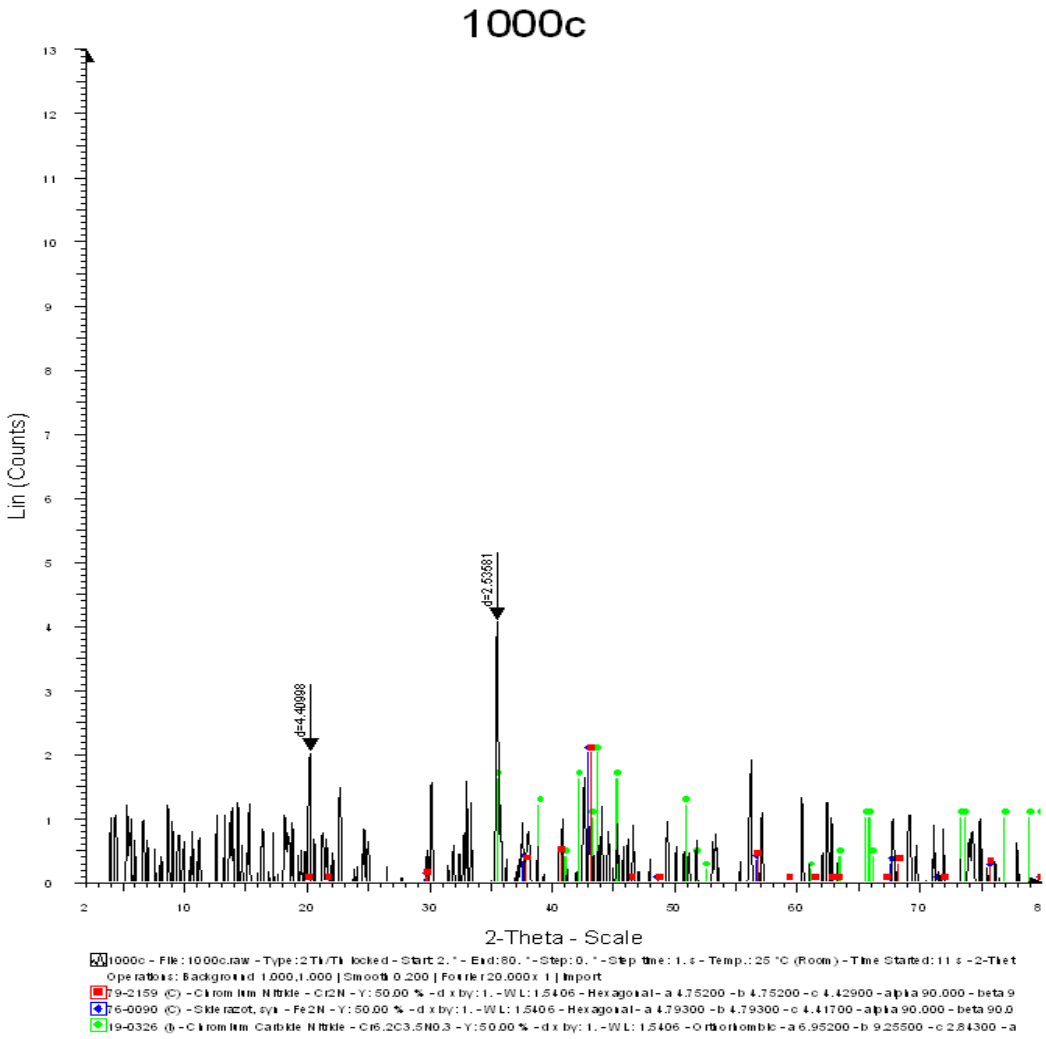

Figure 4.1.7: XRD graph analysis on 1000°C hybrid nitrided sample

Based on the experiment of determining the hardness of the as received sample, 900°C hybrid nitrided sample and 1000°C hybrid nitrided sample, it was found out that the highest hardness value is 478.3 Hv for 900°C hybrid nitriding temperature at 25g Vickers hardness test. While for 1000°C hybrid nitride sample, the highest hardness value is a little less than that at 418.1Hv. Hardness at the same sub-layer was generally higher in the nitride-layer formed at lower temperature, i.e 900°C. This is because the microstructure of the first and second sub-layers, in particular, was much finer and denser at lower temperature. According to this graph, we can see that the distance variable clearly dictates the hardness result (Figure 4.1.8). The hardness value for both 900°C and 1000°C hybrid nitrided samples are highest at the outer core of the samples and the value decreases gradually as it goes deeper into these samples and at certain points, the hardness value stop declining and become constant. This is due to the diffusion capabilities of nitrogen into the sample surface. As the sample get deeper, the harder the nitrogen capability to diffuse and lower nitrogen content were found. Hardness value start to become constant when there is so little or zero nitrogen content in the layer. For the untreated/unnitrided sample, the hardness values are generally constant throughout the sample which due to the consistent microstructure throughout the sample. From the results, they clearly show how the formation of nitrided layer at the sub-surfaces help to increase the hardness value of austenitic stainless steel.

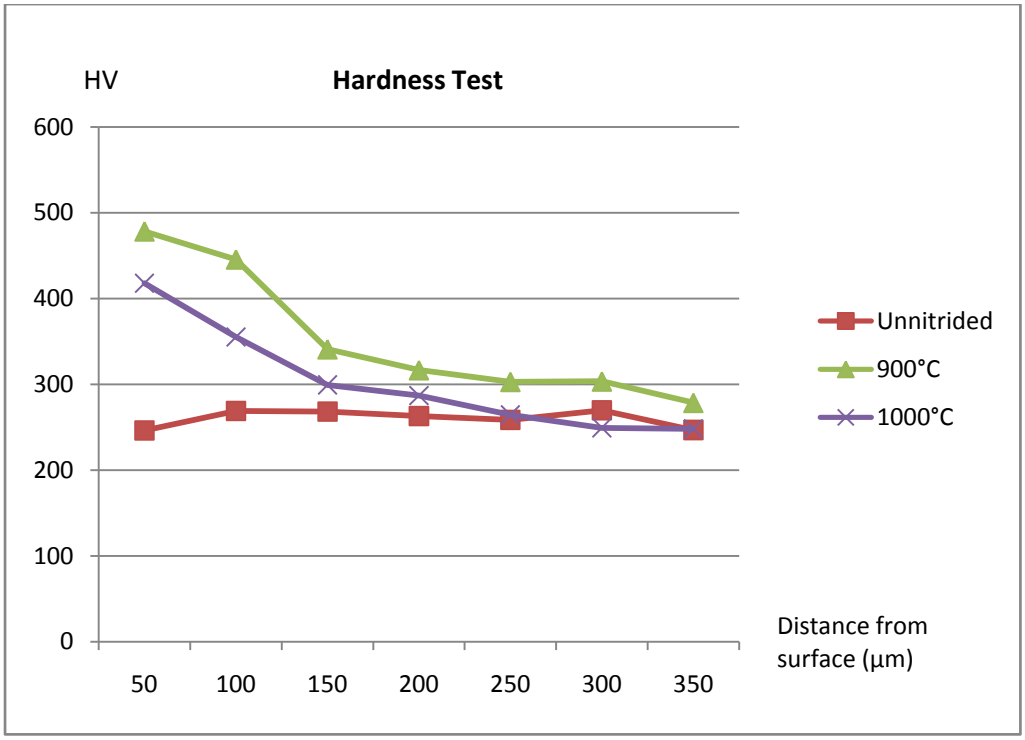

Figure 4.1.8: The graph of 'HV Vs. distance from surface' for unnitrided, 900°C hybrid nitrided and 1000°C hybrid nitrided samples

4.2 Effect of nitriding to AISI 316L ASS at different nitriding methods

Figure 4.2.1 and Figure 4.2.2 compared the microstructure given by 1000°C hybrid nitrided sample and 1000°C conventional nitrided sample. The microstructure analysis of 1000°C hybrid nitrided sample was already given in the first part of result and discussion. For the 1000°C conventional nitrided sample, we can only distinguish the nitrogen diffusion zone into two separated layers. First layer, closest to the surface shows a porous structure associated with fine particles and aggregates. On the second layer, going deeper into the diffusion zone we can see a bulk like structure embedded with fine particles. The nitrogen diffused zone shows S-phase which resulted from the incorporation of excess nitrogen into the austenite phase of the ASS sample.

Comparing the microstructure given by 1000°C hybrid nitrided sample and 1000°C conventional nitrided sample, there is no formation of the unique lamellar structure at 1000°C conventional nitrided sample which can be seen at 1000°C hybrid nitrided sample. It is also obvious that the hybrid nitrided sample shows a deeper nitrogen diffusion zone compared to the conventional nitrided sample. Hybrid nitrided sample has a diffusion depth of 155.1µm while conventional nitrided sample only yield 28.81µm diffusion zone, which means hybrid nitriding improved the diffusivity of the treatment to 538.35%. This clearly shows that hybrid nitriding yield far better results than the conventional nitriding method in term of the ability of nitrogen to diffuse into the sample surface. The presence of carbon given by methane gas during heat treatment helps to multiply the gas diffusion effect on the Austenitic Stainless Steel surface.

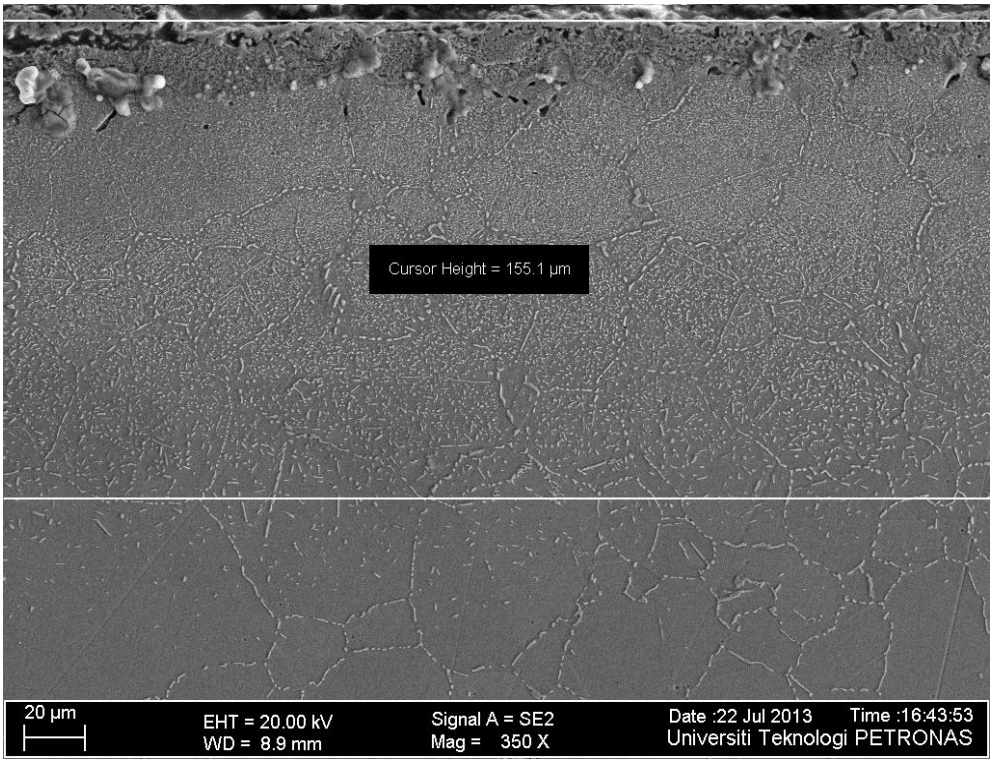

Figure 4.2.1: Microstructure of hybrid nitrided sample at 1000°C using FESEM

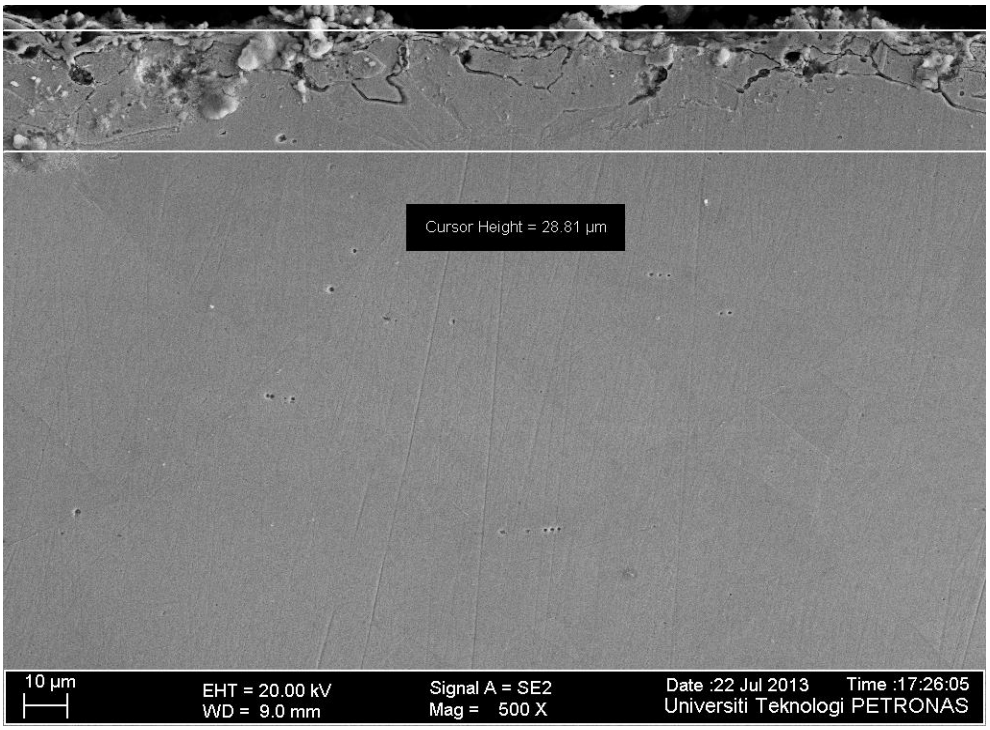

Figure 4.2.2: Microstructure of conventional nitrided sample at 1000°C using FESEM

In order to analyze the ability of the nitriding methods used in the experiments, the weight gain by the samples from the nitriding process were analyze (Table 4.2.1). It is found out that the conventional nitriding process induced 0.002g additional weight to the sample, while 0.009g was induced through hybrid nitriding method. This shows that hybrid nitriding method outweigh the conventional method by 450%. When taken into consideration the surface area of the samples, the weight gain per surface area of conventional nitrided sample and hybrid nitrided sample are $0.000005 g/mm^2$ and $0.0000225 g/mm^2$.

Method	Weight difference (g)	Initial weight (g)	Percentage of weight gain (%)	Weight gain per surface area (g/mm^2)	Treatment diffusion rate (g/s)	Nitrogen diffusion rate (g/s)
Untreated	0	2.368	0	0	0	0
Non-hybrid	0.002	2.359	0.085	0.000005	6.944E-08	6.94E-08
Hybrid	0.009	2.373	0.379	0.0000225	31.25E-08	23.4E-08

Table 4.2.1: Weight gain analysis on different hybrid nitriding methods

From the graph 'weight difference vs nitriding method' (Figure 4.2.3), we can see clearly how the values escalate drastically from conventional nitriding method to hybrid nitriding method. When compared unnitrided sample with the conventional nitrided sample, only 0.002g yielded. But, with only change of nitriding method, the result may improve more than quadruple from the previous one.

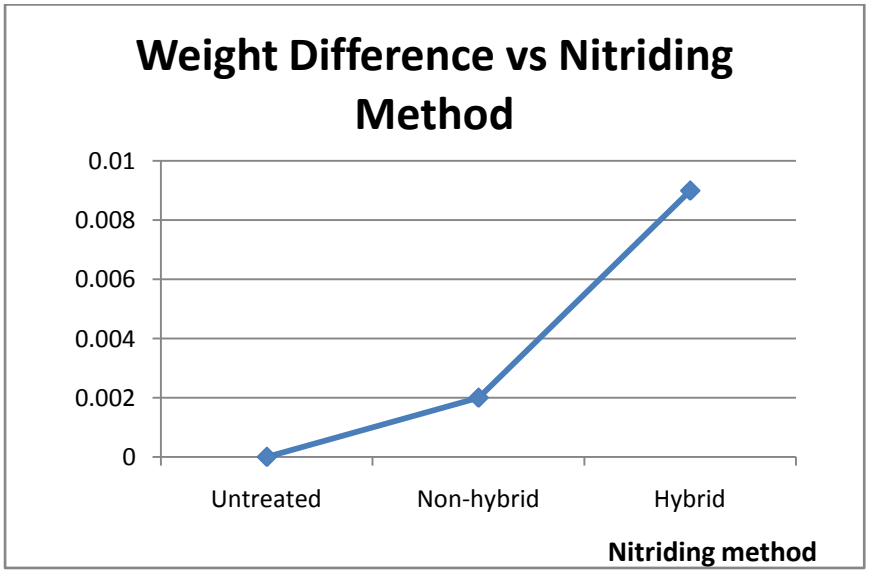

Figure 4.2.3: Graph of 'Weight Difference Vs. Nitriding method'

By taking into consideration the nitriding time, the treatment diffusion rate was calculated. Using 8hours nitriding time (28800s) for both of conventional nitriding and hybrid nitriding methods, treatment diffusion rate are found to be 6.94 x 10^{-8} g/s and 31.25 x 10^{-8} g/s respectively. Graph of 'treatment diffusion rate vs. nitriding method' was drawn (Figure 4.2.4), and as expected, the graph shows same pattern as the previous graph in Figure 4.2.3.

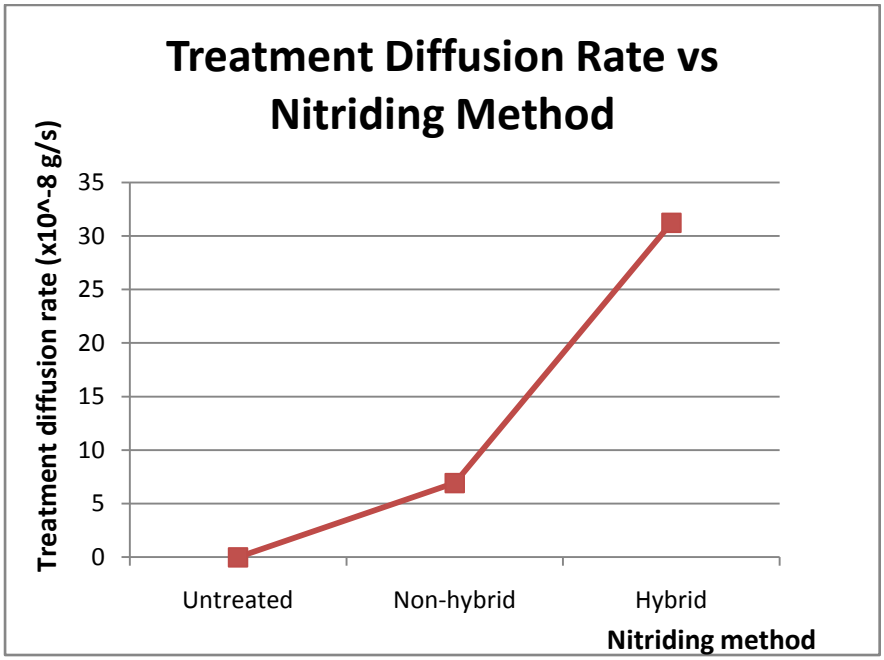

Figure 4.2.4: Graph of 'Treatent Diffusion Rate Vs. Nitriding method'

Figure 4.2.4 shows treatment diffusion rate in general, without considering the gases involved during the treatment. If we only want to focus on the nitrogen, N_2 gas used in the treatment process, a different calculation must be done. Taking consideration the same nitrogen, N_2 flow rate during both of the nitriding processes and only 70% N_2 ratio of the total gas used in the hybrid treatment, a new graph of 'nitrogen diffusion rate vs nitriding method' can be plotted. The graph (Figure 4.2.5) roughly shows the effect of hybrid nitriding method with the presence of ammonia and methane gas, in improving the nitriding effect to the sample's surface. Even after 30% of the weight gain was removed from the calculation, hybrid nitriding method still significantly produced better result when compared to the conventional nitriding method. The nitrogen, N_2 diffusion rate by hybrid nitriding improved more than triple from the result produced by conventional nitriding. Thus, these results shows

that hybrid nitriding by far surpass the conventional nitriding method, improving the nitriding results significantly in term of its nitrogen diffusivity to the austenitic stainless steel surface.

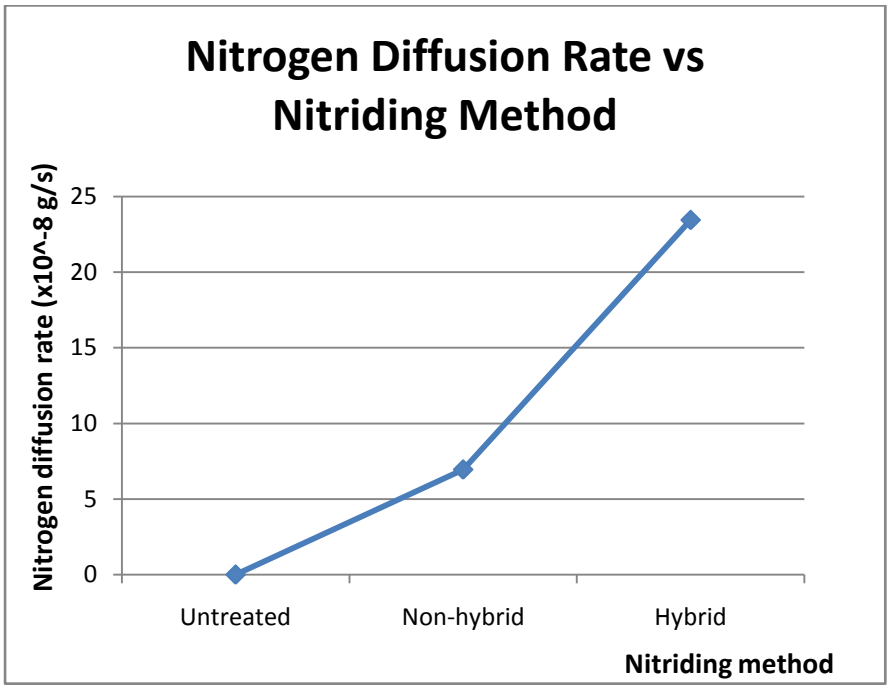

Figure 4.2.5: Graph of 'Nitrogen Diffusion Rate Vs. Nitriding method'

Based on the experiment of determining the hardness of the as received sample, 1000°C hybrid nitrided sample and 1000°C conventional nitrided sample, it was found out that the highest hardness value is 418.1 Hv for 1000°C hybrid nitriding method at 25gf Vickers hardness test (Figure 4.2.6). While for 1000°C conventional nitriding sample, the highest hardness value is at 361.1 Hv which is 13.64% less than hybrid nitrided sample. From the Figure 4.2.6, we can see that the hardness value drops for both the hybrid and conventional nitrided samples as we go deeper into the samples' surfaces with the conventional nitrided sample shows a much steeper gradient. At 2µm, the conventional nitrided samples graph already shows a flat gradient which is due to no nitrogen content found in the sub-layers. While for 1000°C hybrid nitriding method, the hardness test graph show a more constant and less steeper gradient throughout the distance from surface. Only at about 6µm distance from surface, the hybrid nitrided sample shows a constant hardness value which is due to less or zero diffusion of nitrogen into the sub-layer.

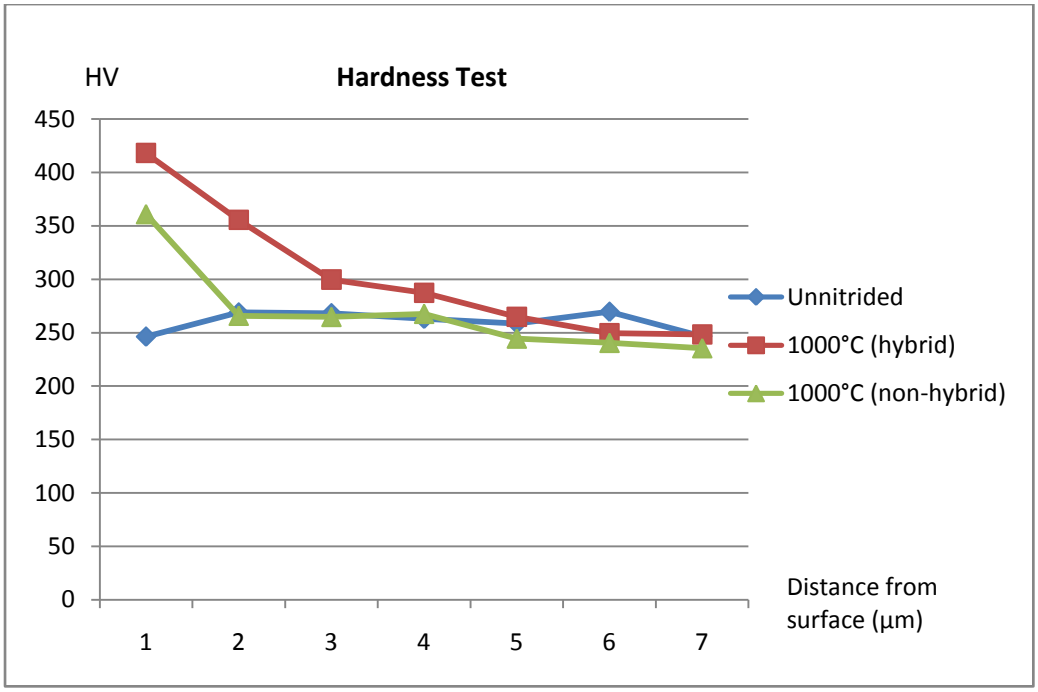

Figure 4.2.6: The graph of 'HV Vs. distance from surface' for unnitrided, 1000°C non-hybrid nitrided and 1000°C hybrid nitrided samples

CHAPTER 5

CONCLUSION AND RECOMMENDATION

5.1 Conclusion

From the above results, conclusion can be derive that nitriding at various high temperatures yielded different and unique outcome with 900°C hybrid nitrided ASS sample shows slightly better surface hardness than 1000°C hybrid nitrided ASS with the highest Hv of the samples are at 478.3Hv and 418.1Hv respectively. Overall, surface hardness of the nitrided samples improved significantly compared to the untreated AISI 316L by more than 65%. From the work, it was also found out that hybrid nitriding which uses additional ammonia and methane gases is better by far than conventional nitriding in term of nitrogen diffusivity by having 500% improvement on the depth of diffusivity zone, 450% increament in weight gain and 15% improvement on the surface hardness.

Some recommendations to further study on the topic ‘ASS high temperature nitriding’ are as follows,

1. Perform high temperature nitriding at even more various temperatures with a wider temperature range

2. Perform nitriding at different hybrid methods – changing the parameters like type of gases to be used and gases ratio composition.

REFERENCES

[1] R. Heidersbach (2011). *Metallurgy and corrosion control in oil and gas production.* New Jersey: John Wiley & Sons Inc.

[2] www.asminternational.org (2008). *Stainless Steels for Design Engineers.*

[3] S. Ren-bo, X. Jian-ying & H. Doug-po (2010). *Characteristics of mechanical properties and microstructure for 316L Austenitic Stainless Steel*

[4] D.Q. Peng, T.H. Kim, J.H. Chung & J.K. Park (2010). *Development of nitride-layer of AISI 304 Austenitic Stainless Steel during high temperature ammonia gas-nitriding*

[5] K.Y. Li & Z.D. Xiang (2009). *Increasing surface hardness of austenitic stainless steels by pack nitriding process.*

[6] N. Tomonori, T. Toshihiro, M. Hiromichi, I. Yukihide & T. Setsuo (2007). *Effect of partial solution nitriding on mechanical properties and corrosion resistance in a type 316L austenitic stainless steel plate.*

[7] Y. Mei (2012). *Nitriding – fundamentals, modeling and process optimization.*

[8] K. Olga (2007). *Fundamentals of Mass Transfer in Gas Carburizing.*

[9] W. Xiaolan (2011). *Activated atmosphere case hardening of steels.*

[10] D. Wu, H. Kahn, G.M. Michal, F. Ernst & A.H. Heuer (2011). *Ferromagnetism in interstitially hardened austenitic stainless steel induced by low-temperature gas-phase nitriding.*

[11] E. Menthe & K.-T. Rie (1999). *Further investigation of the structure and properties of austenitic stainless steel after plasma nitriding*

[12] E. Menthe, A. Bulak, J. Olfe, A. Zimmermann & K.-T. Rie (2000). *Improvement of the mechanical properties of austenitic stainless steel after plasma nitriding*

[13] F. Borgioli, A. Fossati, G. Matassini, E. Galvanetto & T. Bacci (2010). *Low temperature glow-discharge nitriding of a low nickel austenitic stainless steel*

[14] N. Mingolo, A.P. Tschiptschin & C.E. Pinedo (2006). *On the formation of expanded austenite during plasma nitriding of an AISI 316L austenitic stainless steel*

[15] Y. Li, L. Wang, J. Xu & D. Zhang (2011). *Plasma nitriding of AISI 316L austenitic stainless steels at anodic potential*

[16] F.D.S. José, M.G. Carlos & P.T. André (2004). *Improvement of the cavitation erosion resistance of an AISI 304L austenitic stainless steel by high temperature gas nitriding*

[17] W.R. Howie & R.P. Badrak (2010). *Subcritical Carbonitriding For Stainless Steels*

[18] C.X. Li & T. Bell (2003). *Corrosion properties of active screen plasma nitrided 316 austenitic stainless steel*

[19] T. Askar, H. Patthi, H. Esa & I. Mokhtar (2012). *Low Temperature Thermochemical Treatments of Austenitic Stainless Steel Without Impairing Its Corrosion Resistance*

[20] D. Chicot, E.S. Puchi-Cabrera, X. Decoopman, F. Roudet, J. Lesage & M.H. Staia (2011). *Diamond-like carbon film deposited on nitrided 316L stainless steel substrate: A hardness depth-profile modeling*